Ionization of Atoms and Molecules by Electron Impact. Energy Loss and Momentum Transfer

L. V. Sumin and M. V. Gur'ev
All-union Institute of Raw Minerals
Submitted Nov. 15, 1971
Zh. Eksp. Teor. Fiz. 62, 2026–2035 (June, 1972)

We have investigated the momentum transferred to the ion in a collision between electrons and atoms. We have measured the average ion momentum projection $\bar{P}_y$ on the direction of the momentum vector of the ionizing electron. The value of $\bar{P}_y$ is determined by the angular and energy distributions of the knocked-out and scattered electrons, and is connected with the most important characteristics of the collision. At low ionizing-electron energies, the average projection of the ion momentum characterizes the anisotropy of the angular distribution of the secondary electrons. At large electron energies (in the Born approximation), the value of P_y is proportional to the average energy lost by the incoming electron both for the ion and for the excited atom. Data obtained for He, Ne, Ar, Kr, H_2, N_2, CO_2, and H_2O for different electron energies from 30 to 300 eV.

In most experiments on electron-atom collisions with ionization, one measures the differential or total cross-section for the production of an ion with a given charge. The differential cross sections are usually obtained in a limited interval of the angles and energies of the knocked-out electrons. An integral characteristic of the entire distribution function of the electrons with respect to the angles and energies could be the sum of the average momentum projections $\bar{p}_y$ of the scattered and knocked-out electrons on the direction of the momentum p_0 of the incident electron. The collision of a given atom with an incident electron is most conveniently characterized by the quantity $\bar{P}_y = p_0 - \bar{p}_y$ which is the experimentally-measured average projection of the momentum of the ion on the direction of p_0. Preliminary measurements of $\bar{P}_y$ of Ar^+ ions were reported earlier[1]. The experimental data on P_y lend themselves to a simple interpretation at low energies of the incident electrons near the ionization threshold, and at high energies (in the Born approximation).

EXPERIMENTAL PART

The average momentum projections of the atomic and the molecular ions were measured with a setup based on the MB-2302 mass spectrometer (Fig. 1). The gas was fed through tube 1 and ionized in chamber 2. The pressures of the investigated gases in the ionization chamber did not exceed 10^{-4} Torr. The ion beam was shaped with the aid of electrodes 3 and 4 and accelerating electrode 5, with a slit 0.1 mm wide. The ion currents were measured with secondary-electron multiplier 6. We measured the distribution of the ions over the projections of the momentum in the y direction, which was parallel to the mass-analyzer magnetic-field force lines and parallel to the direction of the electron beam. To this end, following Berry[2], a deflecting capacitor was used at the output of the ion source.

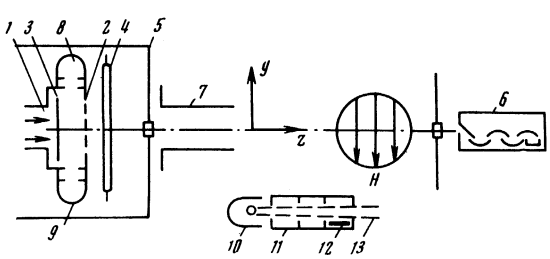

FIG. 1. Diagram of experimental setup.

The aperture of the ion-optical system relative to the y axis was decreased to 0.001, so that only ions with sufficiently low velocity components in the y direction reached the collector. The ions having a certain initial velocity projection in this direction reached the collector if their velocity was compensated for in the deflecting capacitor 7.

A sawtooth voltage from an NGPK-3 generator was applied to the plate of the deflecting capacitor. At a potential difference V (in volts) between the plates, we registered ions having a charge Ze, a mass M, and a momentum projection P_y such that

$$V = (67.5 \pm 2.5) P_y (2mZ)^{-1/2}, \quad (1)$$

where P_y and M are expressed in atomic units ($\hbar = e = m_e = 1$). In calculating the numerical coefficient we took into account the stray field of the deflecting capacitor. It is seen from (1) that the value of V is proportional to the square root of the translational energy transferred to the ion.

The design of the ion-optical system of the ion source was such that acceleration of the ions along the Z axis to an energy 5 keV, for the purpose of mass analysis, did not distort the initial ion velocity in the y direction. To this end, the exit slit of the planar ionization chamber was covered with a grid with a mesh 30 × 30 microns and the ions were extracted from it by a uniform expelling field produced by flat electrode 3. The ion current was amplified and recorded with the EPP-09 electronic potentiometer as a function of the voltage on the deflecting capacitor, i.e., we registered the distribution function of the ions with respect to the projections of the momentum on the y direction. All the measurements were relative. To this end, two electron guns 8 and 9 were placed in the ion source and produced electron beams oriented at an angle 180°. The electron beams 13 were shaped by electrostatic focusing (focusing electrode 10) followed by collimation with two slits 11 each 0.2 mm wide, at a distance 10 mm (Fig. 1).

In the ionization region, the electron beam is deflected in the expelling electric field, so that in order that the beam reach the collector it is necessary to deflect it in the ionization chamber by a certain angle. This was effected by correcting electrode 12. Its potential relative to the cathode, depending on the electron energy and on the intensity of the expelling field, was chosen experimentally to make the electron collector current a maximum (~90% of the total current in the ionization region). The function of electron collector was assumed by the correcting electrode of the "blocked" electron gun. A positive potential (relative to the ionization-chamber slit) sufficient to cause complete gathering of the electrons was applied to the collector. A negative potential was applied to the focusing electrode of the blocked beam. Such a circuit guaranteed the absence of electrons from the "blocked" cathode in the ionization region or at the collector, and made it possible to keep the cathode temperatures constant, an important factor in the stabilization of the thermal regime of the ion source. Special experiments were performed to check that the electron current and the "bulging" of the fields through the slits of the ionization chamber did not affect the measured quantities. The chamber walls were cleaned after 2–5 hours of operation. For control purposes, we measured the thermal energy of the atomic and molecular ions. Accurate to 5–10%, it corresponded to the ionization chamber[3] wall temperature (400–500°K in different experiments), and the energy distribution was Maxwellian down to ~1% of the maximum intensity. Since the atomic and molecular ions have equal kinetic-energy distributions, the apparatus distortions of these distributions are the same for all ions and can therefore be neglected in relative measurements of $\overline{P}_y$. This was confirmed by the reproducibility of the measurements of $\overline{P}_y$ with different (0–50%) apparatus broadening of the experimental distribution curves.

MEASUREMENT METHOD

The average projection of the ion momentum on a specified direction is the first moment of the corresponding distribution function. For a thermal distribution of the atomic and molecular ions, the first moment of the distribution function is equal to 0, i.e., the ion distribution is in this case symmetrical with respect to the zero average velocity projection. When momentum is transferred by the ionizing electron, the ions acquire a momentum increment. We can write

$$f(P_y)=\int_{-\infty}^{\infty}\exp[-\alpha(P-t)^2]\varphi(t)\,dt,$$

where $f(P_y)$ is the experimental distribution function with respect to the momentum projections; $1/\alpha = 2kT/m$ is the square of the most probable momentum of the thermal motion of the atoms and molecules, and $\varphi(P)$ is the distribution function of the ions with respect to the projections of the momentum transferred by the electron. At the maximum we have $f'(P) = 0$, hence

$$P_m=\int_{-\infty}^{\infty}t\varphi(t)\exp\{-\alpha(P_m-t)^2\}\,dt\Big/\int_{-\infty}^{\infty}\varphi(t)\,\exp\{-\alpha(P_m-t)^2\}\,dt. \quad (2)$$

In all cases, the average ion momentum projections were smaller by 1–2 orders of magnitude than the average thermal momentum of the initial atoms and molecules (see Table I), i.e., $P_m\alpha^{1/2} \ll 1$. The exponentials in (2) can therefore be expanded in a series, and after some transformations we obtain

$$P_m=\int_{-\infty}^{\infty}t\varphi(t)\,dt\Big/\int_{-\infty}^{\infty}\varphi(t)\,dt, \quad (3)$$

which is accurate to terms of order αP_m^2. Thus, the position of the maximum of the curve turns out to be equal, with good accuracy, to its first moment, i.e., to the sought value of $\overline{P}_y$, The position of the maximum is easiest to measure since it can be done by registering only the part of the ion distribution in the region of the maximum of the function.

It can be shown that formula (3) is valid not only for a Gaussian curve, but also in a more general case. This explains why the experimentally measured momentum transfer remains practically unchanged in relative measurements even in the presence of considerable apparatus broadening of the registered curve.

The random error arising in the determination of the position of the maximum of the experimental curves includes the following sources: fluctuation of the ion current, instability of the sweep of the deflecting voltage, instability of the speed of the EPP-09 automatic potentiometer chart, and the nonreproducibility of the voltage markers on the plotted experimental curve. The error in the position of the maximum, which includes all the foregoing errors, corresponded in the different experiments to a kinetic-energy transfer 5×10^{-8}–10^{-6} eV.

The experimentally measured position of the maximum of each individual distribution function usually contains a certain additive constant. This constant is connected with the inaccuracy of the mechanical adjustment of the mass spectrometer. To exclude this constant, we measured the relative shift of the average projections of the momenta following a change in the orientation of the electron beam by 180°. Another source of instrument errors is connected with the presence of an electron beam in the ionization chamber. The electrons striking the internal walls of the chamber produce films on which electric charges accumu-

Table I. Experimental values of average ion velocity projection on the electron-impact direction.

Ion	E_0, eV	at. un.	$\Delta\overline{E}+\gamma$, eV	Ion	E_0, eV	at. un.	$\Delta\overline{E}+\gamma$, eV
H_2^+	30	1,38±0.04		He^+	34	1.30±0.12	
	70	0.472±0.10	29		70	1,00±0.07	62
	180	0.195±0.10	19		100	0.70±0.07	52
	500	0.115±0,08	13		140	0.46±0.07	40
	800	0,066±0.015	14		180	0.40±0.1	40
CH_4^+	90	0.28±0.05	25		500	1.16±0.01	26
					800	0.16±0.02	33
$C_6H_{14}^+$	30	1,30±0.15		Ne^+	180	0.94±0.05	93
	70	0,53±0.07	35		500	0.50±0.03	82
	180	0,04±0.05	40		660	0.44±0.03	
N_2^+	500	0,25±0.06	41				
O_2^+	500	0,20±0.06	33	Ar^+	180	0.51±0.15	50
CO_2^+	70	1,15±0.07	71		500	0.29±0.04	48
	500	0,23±0.07	38		800	0.25±0.03	52
H_2O^+	500	0,10±0.05	16	Ar^{++}	180	1.7±0.2	
					460	1.0±0.3	160
				Kr^+	150	0.43±0.1	40
					200	0.40±0.05	42
					460	0,35±0.05	55
					760	0.36±0,05	73
					500	0.42±0.07	69

late and deflect the ions in the y direction (these must not be confused with the contact potential difference). The systematic error introduced by such a field is the same for all ions of like charge, regardless of their mass. To eliminate this error in the relative measurements, we registered the difference between the positions of the maxima of the distributions functions of two ions with different masses. On the other hand, measurement of these differences at two orientations of the electron beams eliminated completely all the systematic measurement errors. The measured quantity was thus the difference between the positions of the maxima of the distribution functions with respect to the momentum projections of two ions with different masses (subscripts i and j) at two different orientations of the electron beams (subscripts a and b):

$$\frac{\bar{P}_{yi}}{(2m_iz_i)^{1/2}} - \frac{\bar{P}_{yj}}{(2m_jz_j)^{1/2}} = \frac{1}{2\cdot 67.5}(V_{ia} - V_{ib} - V_{ja} + V_{jb}).$$

The momenta of the investigated ions were measured relative to xenon ions. To obtain the absolute values of $\bar{P}_{yi}$, the relative experimental values of the momenta were summed with the theoretical value $\bar{P}_y(Xe^+)$ obtained from formulas (11) and (13) (see below). Owing to the large mass of the reference Xe^+ ions, the quantity $V(Xe^+)$ is small and consequently the error in its calculation, which enters in the results for the other ions, is minimal. For example, a factor of 2 change in the calculated value of $V(Xe^+)$ alters the results by not more than 50% for Kr^+ ions (in the worst case), and by 15% for Ar^+.

The absolute values of $\bar{P}_y$ of the H_2^+ ions were determined also by another method. Hydrogen and deuterium were admitted simultaneously and the difference $(V(H_2^+) - V(D_2^+))$ was measured. The momenta of the H_2^+ and D_2^+ ions should be equal, since the electron shells of the molecules H_2 and D_2 are equal, as are the average vibrational energies of the ions, which were calculated by us accurate to several hundredths of an electron volt from the data of[4]. Thus, $\bar{P}_y$ is determined directly from the relation

$$V(H_2^+) - V(D_2^+) = 67.5[\bar{P}_y(2m_2)^{-1/2} - \bar{P}_y(2m_4)^{-1/2}],$$

where m_2 and m_4 are the masses of H_2^+ and D_2^+, respectively. Measurements of the average projection of the momentum of the ions H_2^+ on the y direction with an additional electron beam directed along the x axis (perpendicular to the plane of the figure) have shown that the projection is equal to zero, as it should, within the limits of the measurement errors.

RESULTS AND DISCUSSION

From the momentum conservation law we get for the average projection $\bar{P}_y$ on the direction of the momentum p_0 of the primary electron

$$\bar{P}_y = p_0 - \left(\int p_1 \cos\theta_1\, d\sigma + \int p_2 \cos\theta_2\, d\sigma\right) \Big/ \int d\sigma, \qquad (4)$$

where $d\sigma$ is the differential cross section for the emission of some secondary electron with a definite momentum p; the subscripts 1 and 2 denote the momenta of the fast and slow secondary electrons; θ_1 and θ_2 are the angles between the vector p_0 and the vectors p_1 and p_2. The integration in (4) is over all

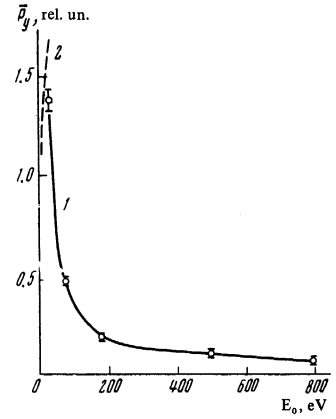

FIG. 2. Average momentum projection of H_2^+ ions vs. the energy of the ionizing electrons. 1—experimental points, 2—calculated curve corresponding to transfer of the total momentum of the ionizing electron.

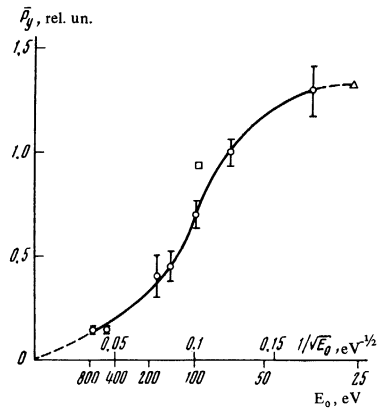

FIG. 3. Average momentum projection of He^+ ions vs. ionizing electron energy: ○—experimental points, □—calculated value from data of [10], Δ—momentum of ionizing electron at $E_0 = 25$ eV.

the phase space of both secondary electrons. If both secondary electrons have isotropic angle distribution, or at least a distribution which is symmetrical with respect to $\theta_{1,2} = 90°$, then it follows directly from (4) that $\bar{P}_y = p_0$, i.e., the ion acquires on the average the momentum of the ionizing electron. An isotropic distribution is obtained at low electron energies E_0 when $E_0 - I \ll I$, where I is the ionization potential[5]. In this case P_y can serve as a measure of the anisotropy of the angular distribution of the secondary electrons. The obtained values of $\bar{P}_y$ of the ions H_2^+ and He^+ (in atomic ions), following ionization by electrons with different energies, are shown in Figs. 2 and 3, respectively. The region of total transfer of the momentum of the impinging electron is seen in both figures at low energies E_0 slightly exceeding the ionization energy. The figures show also plots of $P_y = (2E_0)^{1/2}$.

McKonkey et al.[6] measured the angle of distribution of the ions in the region of low energies E_0. These experiments were performed in only a limited range of angles, and consequently do not show a complete picture of the collision. Detailed measurements such as performed in[6] are impossible at high energies E_0, owing to the strong decrease of the average ion momentum with increasing energy, as is well illustrated in Figs. 2 and 3.

At high electron energies, expression (4) is transformed in the following manner. We introduce the vector $q = p_0 - p_1$. Then

$$p_1 \cos\theta_1 = (p_0^2 + p_1^2 - q^2)/2p_0. \qquad (5)$$

Substituting (5) in (4), we obtain

$$\bar{P}_y = \frac{\Delta\bar{E}}{p_0} + \left(\frac{1}{2p_0}\int q^2 d\sigma - \int p_2 \cos\theta_2 \, d\sigma\right) \Big/ \int d\sigma, \quad (6)$$

$$\Delta\bar{E} = \int (p_0^2 - p_1^2) d\sigma \Big/ 2\int d\sigma,$$

i.e., $\Delta\bar{E}$ is the average energy lost by the incoming electron. Expression (6), like (4), is exact. We denote the second term in (6) by γ/p_0. It turns out to be small at high energies E_0. We estimate its value in the following manner. We subdivide the entire range of variation of q into two regions, $q < q_1$ and $q > q_1$, and apply to them two limiting cases of the Born approximation, corresponding to large and small values of q. At small q ($q < q_1$) we expand $E^{i\mathbf{q}\cdot\mathbf{r}}$ in a series, confining ourselves to the first nonvanishing term of the expansion, and obtain the Bethe approximation

$$d\sigma = \frac{8\pi}{p_0^2} |z|^2 \frac{dq}{q} d\tau_2, \quad (7)$$

where $|z|^2$ is the square of the modulus of the matrix element of the dipole moment of the transition, averaged over all the directions of the moment; $d\tau_2$ is the element of the phase space of the slow electron. We note immediately that at small q, owing to the symmetry of the angular distribution of the "knocked-out" slow electrons, we have $\int p_2 \cos\theta_2 d\sigma = 0$, just as in photoionization.

At large q ($q > q_1$), we regard the atomic electrons as free, and regard the collision with the atom as a collision of the incident of the electron with one of the atomic electrons which is initially at rest[1]. Then

$$d\sigma = 2\pi du / p_0^2 u^2, \quad q^2 = 2u, \quad (8)$$

where u is the energy lost by the incident electron. For a slow secondary electron $\cos\theta_2 = q/p_0$ and $p_2 = [2(u - I)]^{1/2}$, where I is the energy lost to the ionization of the atom and to the excitation of the ion.

Combining (7) and (8), we get

$$d\sigma = \frac{8\pi}{p_0^2} |z|^2 \frac{dq}{q} d\tau_2,$$

$$q_0 < q < q_1, \; d\sigma = \frac{8\pi}{p_0^2}\frac{dq}{q^3}, \quad q_1 < q < q_2. \quad (9)$$

We substitute (9) in (6) and integrate with respect to dq from $q_0 = \Delta\bar{E}/p_0$ to $q = q_2$. The upper limit q_2 is determined from the condition $q_2^2 = E_0$, which corresponds to integration with respect to the energy loss up to $u = 0.5\, E_0$, since the electron energy distribution is symmetrical with respect to $u = 0.5E_0$. We choose q_1 to satisfy the condition $q_1^2 = 2I$. As shown by Gaudin and Rotter[8], such a choice of q_1 ensures an accuracy not worse than 30–50% in the absolute calculation of the ionization cross section by this method. We note that γ depends little on q_2 and q_1. Discarding terms of the order of I/E_0 and $\Delta\bar{E}/E_0$, we obtain

$$\gamma = \frac{2Iz_1 - \ln(E_0/I) + 4 - 3\ln 2}{4z_1 \ln(2(IE_0)^{1/2}/\Delta\bar{E}) + 1/I}. \quad (10)$$

[1]In an earlier calculation[1] we took into account, in essence, only collisions with large orders of q. The calculations of Komsha[7] are in error, and even the sign of $\bar{P}_y$ is incorrect.

Here $z_1 = \int |z|^2 d\tau_2$. In the integration with respect to $d\tau_2$, the slowly-varying logarithmic factor is taken outside the integral sign, using the average value of the energy loss. It is known that $z_1 = 0.5 - 1$ for the outer electrons of practically all atoms ($z_1 \approx 0.3$ for the hydrogen atom), so that averaging over all the electrons of the atom introduces nothing new. We can ultimately write

$$\bar{P}_y = (\Delta\bar{E} + \gamma)/p_0, \quad (11)$$

where γ is a small correction ($\lesssim 0.3$) in the interval $E_0 = 150$–1000 eV. With further increase of E_0 we have $\gamma \to 1/2z_1$. Allowance for the exchange by Ochkur's method[9] in the region of applicability of the Born approximation introduces in (10) only insignificant corrections of the order of I/E_0.

Thus, the quantity $\bar{P}_y$ is directly connected with an important characteristic of the collision, the average energy lost by the incident electron. At the present time there are not enough published experimental data, for a wide scattering-angle interval, from which to determine this quantity. The values of $\Delta\bar{E} + \gamma$ calculated from our data on $\bar{P}_y$ in accordance with formula (11) are listed in the last column of Table I. It is seen from the table that in all cases (with the exception of H_2) $\Delta\bar{E}$ exceeds the ionization potential appreciably. This means that the greater part of the energy lost by the incident electron is transferred to the "knocked-out" electron, and is also consumed in the excitation of the ion. It is of interest to compare the obtained values of $\bar{P}_y$ with other results on the ionization of the atoms and molecules. In particular, it is possible to connect $\bar{P}_y$ with the photoionization cross sections. To this end, we represent $\Delta\bar{E}$ in the form

$$\Delta\bar{E} = \left(\int_{q_0}^{q_1} \Delta E \, d\sigma + \int_{q_1}^{q_2} \Delta E \, d\sigma\right) \Big/ \int d\sigma. \quad (12)$$

We substitute the expressions of (9) in (12) and discard terms of the order of $I/\bar{E}_0$ and $\Delta\bar{E}/E_0$. Further, using (10), we obtain

$$\Delta\bar{E} + \gamma = \left[4\int \Delta E |z|^2 \ln\left(2\frac{(IE_0)^{1/2}}{\Delta E}\right) d\Delta E + 2Iz_1 + 4(1 - \ln 2)\right] \times \left[4\int |z|^2 \ln\left(2\frac{(IE_0)^{1/2}}{\Delta E}\right) d\Delta E + \frac{1}{I}\right]^{-1}. \quad (13)$$

At sufficiently high energies ($E_0 \geq 10^4$ eV), the slowly varying logarithmic factors can be taken outside the integral sign. Then, neglecting the small terms, we obtain a simple expression for the average energy lost by the fast electron

$$\Delta\bar{E} = \int \Delta E |z|^2 d\tau \Big/ \int |z|^2 d\tau. \quad (14)$$

This is equivalent to stating that at high incident-electron energies the principal role is played by collisions with small values of q.

Expression (13) enables us to calculate $\Delta\bar{E} + \gamma$ from photoionization data. We used for this purpose the experimental data on the photoionization cross sections[10]. The results are given in Table II for three values of E_0. For the ions Ar^+ and Kr^+, the difference between the values in Tables I and II greatly exceeds the possible experimental errors. The only substantial error of the theory is apparently the failure to take into account forbidden transitions, the probability of

Table II. Values of $\Delta\overline{E} + \gamma$, calculated from the published data

E_0, eV	Atoms			
	He	Ne	Ar	Kr
200	38	45	20	24
400	39	48	24	24
600	39	50	26	25

which should be small even in the case of electron impact. This question probably deserves further study.

It is interesting that the values of $\overline{P}_y$ are small and decrease with increasing electrode energy. In practice, $\overline{P}_y$ turns out to be equal to the minimum possible value $q = q_0 = \Delta\overline{E}/p_0$, and not to its mean value. Obviously, the greater part of the momentum q is transferred in a direction perpendicular to p_0.[2)] These results should be of certain interest for the study of the mechanism of radiation damage in solids.

The quantity P_y is connected with the angular and energy distributions of the electrons only by the momentum conservation law, so that $\overline{P}_y$ can be used reliably to verify theoretical calculations and the completeness of experimental data on differential cross sections. We know only of one old paper by Goodrich[11], who obtained fairly complete albeit not very accurate angular and energy distributions of the electrons. It follows from a calculation based on Goodrich's data[11] that $\overline{P}_y = 0.9$ for He^+ at $E_0 = 100$ eV. This agrees with our results (see Fig. 3).

An important advantage of the method for measuring the average momentum projection over the usual method of differential cross sections is (besides simplicity) the possibility of separating processes in which ions that differ in charge or in mass are produced (fragment ions of molecular targets). The data obtained by us for the doubly-charged Ar^{++} ions are apparently the only information on the angular and energy distribution of the electrons in such processes. It is seen from Table I that when doubly-charged ions are produced the ionizing electron transfers to the ions a momentum with very large average projection on the impact direction. We can therefore expect to be able to investigate the momentum distribution of doubly-charged ions by the method employed by McKonkey et al.[6] At higher electron energies we can estimate here the energy loss by our method, too, since relation (11) holds for multiply-charged ions regardless of the mechanism whereby they are produced[3)], apart from insignificant modifications of γ.

The expression for the average projection of the target momentum in the case of electron impact has a similar form for elastic as well as all inelastic collisions. In elastic scattering, the average momentum transferred to the atom is $P = p_0\sigma_{tr}/\sigma$, where σ_{tr} and σ are the transport and total collision cross sections, respectively. In the general case, starting from the known formulas (see, for example[14]), we obtain at large E_0 the value $P \approx (b_1/p_0)\ln(b_2 p_0)$, which differs from (11) only in the logarithmic factor (b_1 and b_2 are constants characterizing the atom). For inelastic collisions without ionization, we can likewise readily obtain an expression similar to (11) for allowed as well as forbidden transitions ($z = 0$). In this case the region $q \gg 1$ is of no significance. The expression for γ is, of course, different, but $\gamma \approx 0.1$ as before and decreases with increasing E_0.

The transfer of momentum to the target atom can be used to sort atomic beams or to study the origin of excited atoms or ions. This method was recently used[15] to determine uniquely the mechanism of the process $H_2^+ + H_2 \rightarrow H_3^+ + H$ at low ion energies (~0.1 eV).

[2)]It is easy to show, by a method analogous to that described above, that $\bar{P}_x^2 \approx 0.3$ and decreases weakly (logarithmically) with increasing E_0.

[3)]Van der Wiel and Wiebes[12,13] obtained, by a coincidence method, data on the energy loss at small values of q in collisions between electrons having $E_0 = 10^4$ eV and Ar, He, and Ne atoms, including processes in which multiply charged ions are produced.

[1]L. V. Sumin, M. V. Gur'ev, and N. N. Tunitskiĭ, Zh. Eksp. Teor. Fiz. **47**, 452 (1964) [Sov. Phys.-JETP **20**, 299 (1965)].
[2]C. Berry, Phys. Rev. **78**, 597 (1950).
[3]V. L. Tal'roze and E. L. Frankevich, Zh. Eksp. Teor. Fiz. **26**, 497 (1956).
[4]H. Dunn, J. Chem. Phys. **44**, 2592 (1966).
[5]H. S. W. Massey and E. H. S. Burhop, Electronic and Ionic Impact Phenomena, Oxford, 1952.
[6]J. W. McConkey, W. R. Newell, and A. Crowe, J. Phys. B **3**, L55 (1970).
[7]G. Komsha, Izv. Akad. Nauk SSSR Ser. Fiz. **30**, 2008 (1966).
[8]A. Gaudin and R. Rotter, J. Chem. Phys. **65**, 1112 (1968).
[9]V. I. Ochkur, Zh. Eksp. Teor. Fiz. **47**, 1746 (1964) [Sov. Phys.-JETP **20**, 1175 (1965)].
[10]J. A. R. Samson, in: Adv. Atom. Mol. Phys., ed. by D. R. Bates and I. Esterman, Academic, Vol. 2, 1966, p. 177.
[11]M. Goodrich, Phys. Rev. **52**, 259 (1937).
[12]M. J. Van Der Wiel and G. Wiebes, Physica (Utr.) **53**, 225 (1971).
[13]M. J. Van Der Wiel and G. Wiebes, Physica (Utr.) **54**, 411 (1971).
[14]L. D. Landau and E. M. Lifshitz, Kvantovaya mekhanika (Quantum Mechanics) IIL, 1963 [Addison-Wesley, 1965].
[15]L. V. Sumin and M. V. Gur'ev, Dokl. Akad. Nauk SSSR **193**, 858 (1970).

Translated by J. G. Adashko
235